ACS Photonics

Article

pubs.acs.org/journal/apchd5

Nanoplasmonic Filters for Hollow Core Photonic Crystal Fibers

Peter Reader-Harris* and Andrea Di Falco*

SUPA, School of Physics and Astronomy, University of St Andrews, North Haugh, St Andrews, KY16 9SS, United Kingdom

ABSTRACT: We demonstrate a method to add photonic functionalities to the tip of hollow photonic crystal fibers, for ultracompact and integrated lab-on-fiber applications. Specifically we present an angularly robust passband filter that is directly applied to the facet of a fiber, without adhesive or etching. The filter exploits the engineered plasmonic response of metallic features realized on a polymeric membrane and works over a range of 10 degrees, with a passband of 50 nm, centered at a wavelength of 800 nm. This result extends the available functionalities offered by the lab-on-fiber methodology to photonic crystal fibers, as well as providing a reversible method of functionalizing any type of fiber.

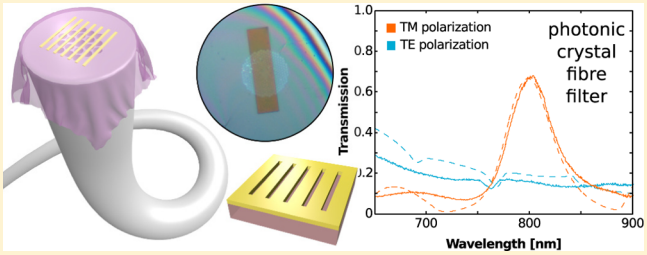

KEYWORDS: *lab-on-fiber, photonic crystal fibers, flexible photonics, surface plasmon resonances*

Optical fibers are a long-established technology for light transport, but are increasingly being used for more exotic purposes, to take fibers beyond point-to-point light delivery. Various ways to introduce additional functionality to fibers exist, including the well-established techniques of fiber Bragg gratings and photonic crystal fibers (PhCF). The latter, in particular, have become extremely useful photonic elements, as they combine accurate light dispersion management with high field localization. PhCF have been used for very high numerical aperture devices,[1] single-mode operation at all wavelengths,[2] and polarization control.[3,4] In addition, PhCF are ideal candidates for strong nonlinear processes such as the generation of supercontinuum light,[5,6] as well as the propagation of solitons.[7] A peculiar type of fiber is the hollow core photonic crystal fiber (HCPhCF). In this case, light is confined in air by reflection from the band gap of an array of holes surrounding the hollow light-guiding region.[8] This type of fiber is particularly useful in sensing applications,[9] with either gases or liquids flowing through the hollow sections. Sensing can be performed by a number of different methodologies, including near-infrared (NIR) absorption spectroscopy[10] and fluorescence spectroscopy,[11] where the light signal is coupled from the fiber into a number of external components that process the signal. Integrating these often bulky components directly on the fibers could increase the portability and practical impact of PhCF sensors at reduced costs.

An elegant solution to this requirement is offered by the lab-on-fiber (LoF) approach. This emerging technology is a complementary method for the control of light behavior in fibers, adding functionality to their surface, usually the facet.[12,13]

LoF fabrication techniques can be classified into the transfer method[14] and the direct writing method.[15] The latter uses the same lithographic processes to define nanofeatures on planar wafer substrates, adapted to more challenging topology of the fiber tip. The transfer method decouples the choice of fiber and the method of fabrication, by realizing the functional element separately from the fiber and then combining them later. Flexible photonic membranes[16−19] are exceptionally well suited for this task, as they are compliant to the fiber facet, are free-standing, can be easily replaced, and can be made cheaply. Examples of the opportunities arising from these unique properties include rolled up multilayers,[20] the fabrication of nanoapertures in a flexible membrane,[21] stretch tuning,[22] and flexible negative refractive index materials.[23]

In this paper we present the use of flexible photonic membranes as a general method to reversibly functionalize the facet of any type of fiber, including where the facet is “just air”, as in the case of HCPhCF.

Specifically, we focus on a design inspired by the guided mode resonance (GMR) filter, based on the interaction of light confined in a waveguide with an adjacent grating. In our case the membrane itself acts as a waveguide, whereas the grating is realized by patterning an overlaying gold layer, supporting surface plasmon polaritons (SPPs). This coupling can create narrow line width filters,[24] typically at the cost of a strong angular dependence. This issue can be solved by mounting the filter on top of a fiber collimator,[19] although this implementation reduces the compactness of the filter. Alternative published methods for creating angularly robust GMR-type filters at telecom wavelengths use doubly periodic grating systems on a multilayer.[25] A theoretical investigation with a doubly periodic structure incorporating a grating on both sides of the membrane has shown similar results in the mid-IR.[26]

Here we present a solution based on a single-period grating, which is angularly robust enough to filter efficiently a fiber with a numerical aperture (NA) of 0.17 (10 degrees).

Received: June 18, 2014
Published: September 16, 2014

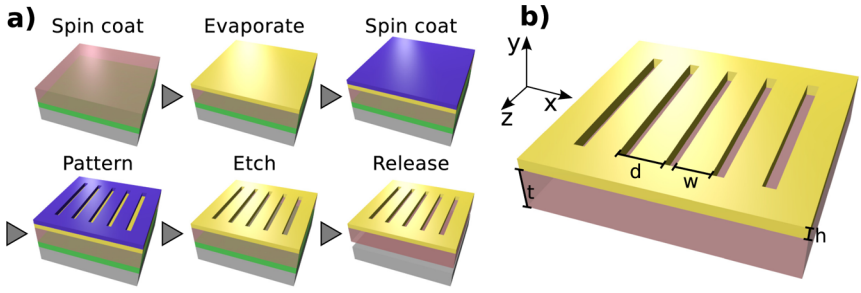

Figure 1. (a) Sketch of the fabrication protocol. (b) Sketch of the final membrane with relevant geometrical parameters.

Remarkably, our filter is the simplest among the whole family of metasurfaces,[27] but demonstrates that the platform is a robust way to create an arbitrary photonic response on the tips of photonic crystal fibers, thus bringing a new design paradigm to the field.

RESULTS

The membrane was fabricated with the process illustrated in Figure 1a. A sacrificial layer and a polymer layer are deposited via spin coating on a rigid substrate, followed by the evaporation of a layer of metal. A positive tone photoresist is patterned via electron beam lithography, and this pattern is transferred into the gold via reactive ion etching. Finally, the sacrificial layer between the substrate and the membrane is dissolved and the membrane is released. If necessary, the membrane can be mounted onto another object or a frame. The fabrication details can be found in the Methods section. Figure 1b shows the relevant geometrical parameters, with a typical membrane thickness of 260 nm and gold thickness of 40 nm. On the metal we engraved an array of slits of 150 nm width and periodicity of 600 nm. However, the fabrication and manipulation protocol used here is not specific to this pattern. We have fabricated membranes in this fashion with different patterns, as well as with continuous gold and without any gold.

The band structure relative to our geometry is shown in Figure 2b, as calculated by a finite element analysis package, for both TE (electric field parallel to the z axis, red open circles) and TM polarizations (magnetic field parallel to the z axis, black solid circles). The TE band structure does not support surface plasmons and was reported for completeness. Additionally, the TE modes of the waveguides can be tuned fairly independently of the TM resonances by changing the thickness of the membrane alone. To implement an angularly robust filter, we require a flat band structure for a range of wavevectors around the normal incidence value (k = 0), at the operation wavelength. This can be obtained by engineering the anticrossing of the bands of the supported states.[28] The symmetry of the bands is crucial to determine the coupling efficiency of light incident on the filter.[29] Figure 2a shows the y-component of the electric field in the xy plane for two contiguous bands in the working wavelength region. Light incident on the sample couples efficiently only to the antisymmetric band centered at 800 nm, whereas the coupling to symmetric bands (higher and lower frequencies) is not as efficient.

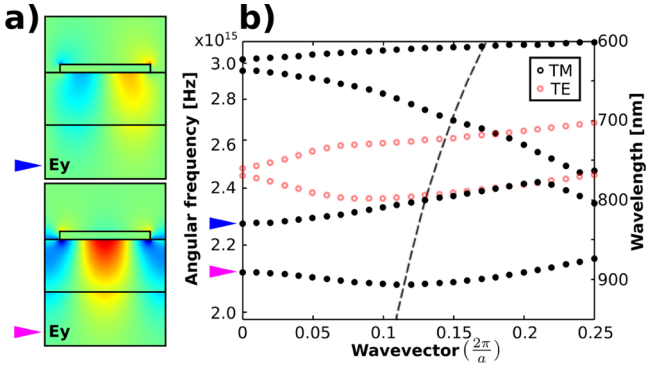

Figure 2. (a) The electric field profile (Ey) for the antisymmetric (top, blue arrow) and symmetric (bottom, pink arrow) bands at k = 0. (b) Band structure for the fabricated sample for TE (red open circles) and TM (black solid circles) polarizations. The dotted line shows the wavevector for each wavelength corresponding to 10° incidence from normal.

This is also confirmed by the angularly resolved transmission spectra for the TM polarization shown in Figure 3. The simulated transmission map (panel a), obtained with rigorous coupled wave analysis (RCWA), coincides with the experimental data (panel b), obtained on the free-standing membrane. The transmission map is in perfect agreement with the band structure of Figure 2 and shows excellent angular robustness at 800 nm, which is sufficient to accommodate the NA of the chosen HCPhC fiber. In Figure 2 we marked the incident angle of 10° with a dashed line, as a guide for the eye.

The filter membrane was then mounted on the tip of the fiber as sketched in Figure 4a. A small PDMS collar was fabricated using an empty fiber ferrule. This assembly allowed the sample to be placed in direct contact with the fiber facet reversibly, so that the same membrane could be used on different fibers. The patterned area of the photonic membrane was centered on the collar with a micropositioner. The membrane was in contact only with the collar and fiber during the measurements, as in the figure. If required, the membrane could be glued permanently in place. Figure 4b shows an optical micrograph of a typical membrane being applied to a photonic crystal fiber, the facet of which is shown in the scanning electron microscope (SEM) image shown in panel c. Panel d shows a SEM image of the nanoslit grating. The interference fringes on the top right of panel b are caused by a fiber facet that is not completely planar, possibly due to imperfect cleaving, which prevents perfect contact with the membrane on the corner. Remarkably, the flexible nature of the membrane permits anyway a good contact on the core area of the fiber, despite the nonplanar facet.

The passband of the filter was centered at 800 nm, to overlap with the transmission band of the used HCPhCF. The resulting transmission spectrum, normalized to the spectrum from the unfiltered fibers, is shown in Figure 5, along with RCWA simulations for the same filter geometry, taking into account

dx.doi.org/10.1021/ph500222w | ACS Photonics 2014, 1, 985−989

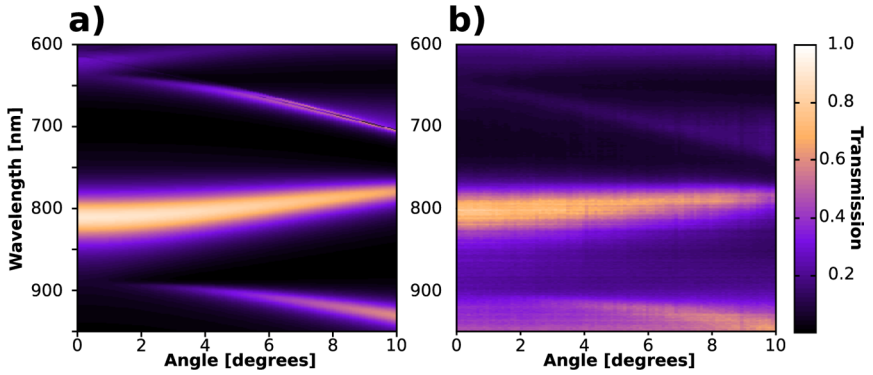

Figure 3. (a) RCWA simulation of the angularly resolved transmission spectrum of the filter. (b) The experimentally measured angularly resolved transmission spectrum.

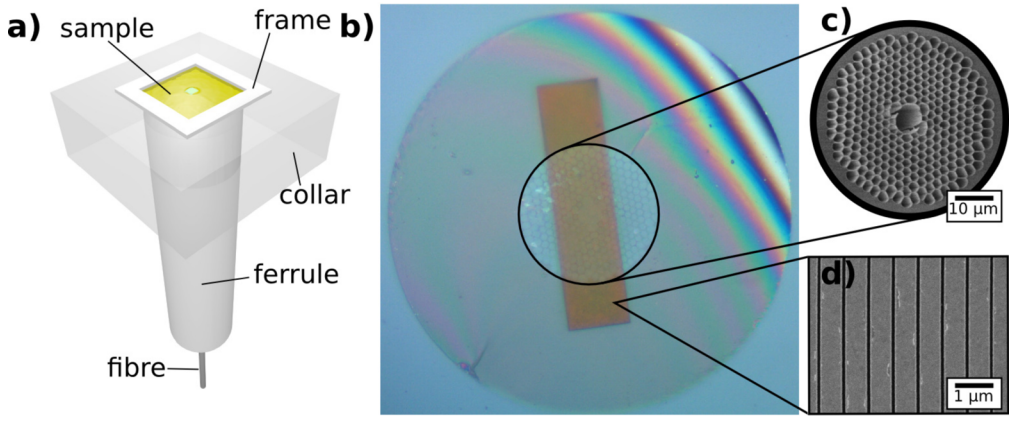

Figure 4. (a) Assembly of the complete lab-on-fiber structure. (b) Optical micrograph of the HCPhCF with a gold nanostructured membrane applied. (c) SEM picture of the HCPhCF facet used. (d) SEM picture of the gold nanoslit grating.

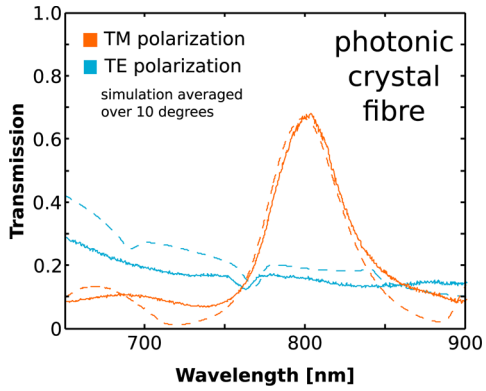

Figure 5. Measured transmission spectrum for both TE and TM polarization as mounted on two types of optical fiber (solid), overlaid with RCWA simulation, taking into account the spread of angles from the fiber (dashed).

the range of input angles. Using the angular spread as a fitting parameter, we found that the RCWA simulations fitted best for a spread of 10 degrees, which corresponds to an NA of the fiber of 0.17. The resonance has a full-width at half-maximum (fwhm) of 51 nm. This design also permits polarization control, with the SPPs coupling with TM light. The small dip in the TE transmission spectrum, at 760 nm, is caused by the small band gap shown in the TE band structure (red) of Figure 2. Using a thicker gold layer increases the polarization contrast, although at the possible expense of increased losses.

From a practical point of view, we note that despite the complete filter being less than 300 nm thick, the membrane does not require any special handling procedures beyond that of standard optical components, once mounted into the frame. Once framed, we used a micropositioner to align the patterned area of the membrane with the core of the fiber. Patterning a larger area of the membrane could trivially lift this requirement. The fabrication yield of the flexible metasurface is practically 100%, and mounting the fiber into a ferrule prevents the membrane from being pierced during assembly. The filter is reusable and can be transferred from fiber to fiber, without observable loss of performance.

DISCUSSION

The use of flexible photonic membranes for lab-on-fiber applications has a number of desirable properties. The transfer of a flexible membrane enables a good contact onto the fiber facet, without reliance on adhesive or van der Waals forces. Rigid photonic crystals have been transferred onto a fiber facet, using epoxy as a glue,[30] but this is essentially irreversible. Our approach grants the reusability of the membrane and of the fiber, which is not permanently modified by the application of the filter. However, it is possible to wrap permanently the membrane at the end of the fiber, thus without using the frame, ferule, and PDMS collar.

In order to create angular robustness in the GMR-type filter, we used metal, thus introducing losses that are detrimental from a bandwidth point of view. A possible solution is to replace the metal with a high-index dielectric, while retaining

dx.doi.org/10.1021/ph500222w | ACS Photonics 2014, 1, 985−989

the flexible nature of the substrate, possibly using a photonic crystal design. However, it is typically easier to get the large anticrossing required to generate angular robustness with SPP-type propagation than with all-dielectric waveguide systems. Additionally it is easier to conceive scaling up the fabrication of metal-based flexible filters than their all-dielectric counterparts.

HCPhCF have the unique ability to pass fluids through the hole that runs their length, enabling a new pathway for LoF integration into sensing experiments. An example of this is surface-enhanced Raman spectroscopy (SERS), which has been demonstrated with a hollow core photonic crystal fiber as the substrate.[31,32] A filter could be usefully employed to eliminate the pump light from the transmitted beam in such a SERS experiment, which would be a step forward to a compact, integrated system for SERS, rather than the bulky apparatus used today. Additionally, in HCPhCF the shape of the flexible fiber mounted device could be tailored by varying the applied pressure of fluid in the fiber, thus tuning the LoF properties.

The filter presented here is just one example of the flexible photonic membrane platform. Other applications could include fiber-mounted optomechanics or beam shaping. In the case of optomechanical systems, light from the fiber can create vibrational modes in the ultrathin membrane by radiation pressure. Direct beam shaping of a fiber's output is a possibility with patterned surfaces, as has already been demonstrated in free space at NIR frequencies.[33,34] Generating the desired eigenmode straight from the fiber, including Bessel beams or orbital angular momentum modes, could create new applications for optical trapping or coupling to external devices. Structured fiber facets have already shown their use in endoscopy,[35] and we see the ability to reversibly add sensing, and other, elements to endoscopes as a key area for a lab-on-fiber to impact.

CONCLUSION

We have demonstrated a fabrication protocol to functionalize the facet of any fiber. This permits merging the promising potential of the lab-on-fiber protocol to the already rich physics of hollow photonic crystal fibers. We have shown the versatility of this technique by creating a reusable angularly robust spectral filter. This result could lead to the demonstration of a new class of compact, integrated fiber-based devices.

METHODS

Band-Structure Simulation. The simulation of the band structure of periodic metallic nanostructures is typically complicated in the IR/visible regime by the highly dispersive metal response. To compute the band structure, we used a wave vector marching technique on COMSOL Multiphysics. We started by calculating the eigenfrequencies at $k = 0$ and used them as the initial inputs to calculated the eigenmodes for small increments of k. As long as the steps in k are small enough, the dispersion in the optical constants can be assumed to be small.

Device Fabrication. The flexible photonic membrane was fabricated according to a method adapted from ref 16. A silicon wafer was used to provide the rigid, planar support for the fabrication steps. It was spin coated with Omnicoat, a release layer from Microchem Corp., at 1000 rpm and baked at 230 °C for 1 min. Then a diluted epoxy-based polymer (SU8 2000.5, from the same company, 1:2 in cyclopentanone) was spun to a thickness of about 260 nm at a speed of 1000 rpm, before baking at 100 °C for 5 min. The SU8 was then cured for 2 min with ultraviolet light and baked at 100 °C for a further 2 min. A 40 nm thick gold layer was then evaporated with an electron beam evaporator and patterned via electron beam lithography (30 kV with a dose of 800 pAs/cm) using ZEP520A, from Zeon Corp., as photoresist, spun at 5000 rpm, and baked for 20 min at 140 °C. Xylene at 23 °C was used to develop the ZEP520A for 45 s. Etch back was then achieved with an argon plasma in a reactive ion etcher, for 9 min at a dc bias of −333 V. Any leftover ZEP was cleaned by trichloroethylene in an ultrasonic bath. The initial Omnicoat layer was then released using *N*-methyl-2-pyrrolidone at 60 °C. The membrane was then transferred to a water bath, where it could be hydrophobically suspended on the water's surface, and subsequently manipulated or mounted into a frame or onto another object.

Sample Measurement. The samples were measured first in a free-standing configuration in order to get the angularly resolved spectrum of Figure 2b. The sample was directly illuminated by a polarized Koheras SuperK Compact supercontinuum laser. An objective was used to image the sample in transmission onto a punctured screen, such that the light illuminating the patterned area of the sample went through to an Ocean Optics 2000+ USB spectrometer. For the spectra in Figure 5, the sample was then mounted onto the fiber and collar by a micrometer drive, and the fiber was illuminated at one end by an unpolarized halogen lamp source. The sample-coated end was imaged with a 20× objective into an Ocean Optics 2000+ USB spectrometer. A polarizer was placed between the objective and the spectrometer, so as to observe the polarization dependence of the filter. In both cases (free space and fiber measurements) the normalization spectra were taken for both polarizations with the same setup without the sample present. The fiber used was a hollow core photonic crystal fiber from NKT Photonics: HC-800-02.

AUTHOR INFORMATION

Corresponding Authors

*(P. Reader-Harris) E-mail: pjrh@st-andrews.ac.uk. Phone: +44 (0)1334 463165. Fax: +44 (0)1334 463104.

*(A. Di Falco) E-mail: adf10@st-andrews.ac.uk.

Notes

The authors declare no competing financial interest.

ACKNOWLEDGMENTS

The authors acknowledge support from EPSRC (EP/I004602/1).

REFERENCES

(1) Wadsworth, W.; Percival, R.; Bouwmans, G.; Knight, J.; Birks, T.; Hedley, T.; Russell, P. St. J. Very high numerical aperture fibers. *IEEE Photonics Technol. Lett.* **2004**, *16*, 843−845.

(2) Birks, T. A.; Knight, J. C.; Russell, P. St. J. Endlessly single-mode photonic crystal fiber. *Opt. Lett.* **1997**, *22*, 961−963.

(3) Suzuki, K.; Kubota, H.; Kawanishi, S.; Tanaka, M.; Fujita, M. Optical properties of a low-loss polarization-maintaining photonic crystal fiber. *Opt. Express* **2001**, *9*, 676−680.

(4) Kubota, H.; Kawanishi, S.; Koyanagi, S.; Tanaka, M.; Yamaguchi, S. Absolutely single polarization photonic crystal fiber. *IEEE Photonics Technol. Lett.* **2004**, *16*, 182−184.

(5) Dudley, J. M.; Genty, G.; Coen, S. Supercontinuum generation in photonic crystal fiber. *Rev. Mod. Phys.* **2006**, *78*, 1135−1184.

(6) Travers, J. C.; Rulkov, A. B.; Cumberland, B. A.; Popov, S. V.; Taylor, J. R. Visible supercontinuum generation in photonic crystal

fibers with a 400 W continuous wave fiber laser. *Opt. Express* **2008**, *16*, 14435−14447.
(7) Travers, J. C. Blue solitary waves from infrared continuous wave pumping of optical fibers. *Opt. Express* **2009**, *17*, 1502−1507.
(8) Cregan, R. F.; Mangan, J. C.; Knight, J.; Birks, T.; Russell, P. St. J.; Roberts, P. J.; Allan, D. C. Single-Mode Photonic Band Gap Guidance of Light in Air. *Science* **1999**, *285*, 1537−1539.
(9) Cubillas, A. M.; Unterkofler, S.; Euser, T. G.; Etzold, B. J. M.; Jones, A. C.; Sadler, P. J.; Wasserscheid, P.; Russell, P. St. J. Photonic crystal fibres for chemical sensing and photochemistry. *Chem. Soc. Rev.* **2013**, *42*, 8629−8648.
(10) Ritari, T.; Tuominen, J.; Ludvigsen, H.; Petersen, J.; Sørensen, T.; Hansen, T.; Simonsen, H. Gas sensing using air-guiding photonic bandgap fibers. *Opt. Express* **2004**, *12*, 4080−4087.
(11) Cordeiro, C. M. B.; dos Santos, E. M.; Brito Cruz, C. H.; de Matos, C. J.; Ferreira, D. S. Lateral access to the holes of photonic crystal fibers - selective filling and sensing applications. *Opt. Express* **2006**, *14*, 8403−8412.
(12) Reader-Harris, P.; Di Falco, A. Functional Metamaterials for Lab-on-Fiber. In *Lab-on-Fiber Technology*; Cusano, A., Consales, M., Crescitelli, A., Ricciardi, A., Eds.; Springer Series in Surface Sciences; Springer: Geneva, 2015; Vol. *56*, pp 111−132.
(13) Consales, M.; Pisco, M.; Cusano, A. Lab-on-fiber technology: a new avenue for optical nanosensors. *Photonic Sensors* **2012**, *2*, 289−314.
(14) Smythe, E. J.; Dickey, M. D.; Whitesides, G. M.; Capasso, F. A technique to transfer metallic nanoscale patterns to small and non-planar surfaces. *ACS Nano* **2009**, *3*, 59−65.
(15) Ricciardi, A.; Consales, M.; Quero, G.; Crescitelli, A.; Esposito, E.; Cusano, A. Lab-on-fiber devices as an all around platform for sensing. *Opt. Fiber Technol.* **2013**, *19*, 772−784.
(16) Di Falco, A.; Ploschner, M.; Krauss, T. F. Flexible metamaterials at visible wavelengths. *New J. Phys.* **2010**, *12*, 113006.
(17) Lipomi, D. J.; Martinez, R. V.; Kats, M. A.; Kang, S. H.; Kim, P.; Aizenberg, J.; Capasso, F.; Whitesides, G. M. Patterning the tips of optical fibers with metallic nanostructures using nanoskiving. *Nano Lett.* **2011**, *11*, 632−636.
(18) Di Falco, A.; Zhao, Y.; Alù, A. Optical metasurfaces with robust angular response on flexible substrates. *Appl. Phys. Lett.* **2011**, *99*, 163110.
(19) Reader-Harris, P.; Ricciardi, A.; Krauss, T. F.; Di Falco, A. Optical guided mode resonance filter on a flexible substrate. *Opt. Express* **2013**, *21*, 1002−1007.
(20) Kolle, M.; Zheng, B.; Gibbons, N.; Baumberg, J. J.; Steiner, U. Stretch-tuneable dielectric mirrors and optical microcavities. *Opt. Express* **2010**, *18*, 4356−4364.
(21) Cho, H.; Kim, J.; Park, H.; Won Bang, J.; Seop Hyun, M.; Bae, Y.; Ha, L.; Yoon Kim, D.; Min Kang, S.; Jung Park, T.; et al. Replication of flexible polymer membranes with geometry-controllable nano-apertures via a hierarchical mould-based dewetting. *Nat. Commun.* **2014**, *5*, 3137.
(22) Pryce, I. M.; Aydin, K.; Kelaita, Y. A.; Briggs, R. M.; Atwater, H. A. Highly strained compliant optical metamaterials with large frequency tunability. *Nano Lett.* **2010**, *10*, 4222−4227.
(23) Chanda, D.; Shigeta, K.; Gupta, S.; Cain, T.; Carlson, A.; Mihi, A.; Baca, A. J.; Bogart, G. R.; Braun, P.; Rogers, J. A. Large-area flexible 3D optical negative index metamaterial formed by nanotransfer printing. *Nat. Nanotechnol.* **2011**, *6*, 402−407.
(24) Wang, S. S.; Magnusson, R. Theory and applications of guided-mode resonance filters. *Appl. Opt.* **1993**, *32*, 2606−2613.
(25) Fehrembach, A.-L.; Talneau, A.; Boyko, O.; Lemarchand, F.; Sentenac, A. Experimental demonstration of a narrowband, angular tolerant, polarization independent, doubly periodic resonant grating filter. *Opt. Lett.* **2007**, *32*, 2269−2271.
(26) Sakat, E.; Héron, S.; Bouchon, P.; Vincent, G. Metal-dielectric bi-atomic structure for angular-tolerant spectral filtering. *Opt. Lett.* **2013**, *38*, 425−427.
(27) Kildishev, A. V.; Boltasseva, A.; Shalaev, V. M. Planar photonics with metasurfaces. *Science* **2013**, *339*, 1232009.
(28) Gao, H.; Zhou, W.; Odom, T. W. Plasmonic crystals: a platform to catalog resonances from ultraviolet to near-infrared wavelengths in a plasmonic library. *Adv. Funct. Mater.* **2010**, *20*, 529−539.
(29) Enkrich, C.; Wegener, M.; Linden, S.; Burger, S.; Zschiedrich, L.; Schmidt, F.; Zhou, J. F.; Koschny, T.; Soukoulis, C. Magnetic metamaterials at telecommunication and visible frequencies. *Phys. Rev. Lett.* **2005**, *95*, 203901.
(30) Shambat, G.; Provine, J.; Rivoire, K.; Sarmiento, T.; Harris, J.; Vučković, J. Optical fiber tips functionalized with semiconductor photonic crystal cavities. *Appl. Phys. Lett.* **2011**, *99*, 191102.
(31) Yan, H.; Gu, C.; Yang, C.; Liu, J.; Jin, G.; Zhang, J.; Hou, L.; Yao, Y. Hollow core photonic crystal fiber surface enhanced Raman probe. *Proc. SPIE* **2007**, *6433*, 643307.
(32) Yang, X.; Shi, C.; Newhouse, R.; Zhang, J. Z.; Gu, C. Hollow-core photonic crystal fibers for surface-enhanced raman scattering probes. *Int. J. Opt.* **2011**, *2011*, 1−11.
(33) Pfeiffer, C.; Grbic, A. Cascaded metasurfaces for complete phase and polarization control. *Appl. Phys. Lett.* **2013**, *102*, 231116.
(34) Pfeiffer, C.; Emani, N. K.; Shaltout, A. M.; Boltasseva, A.; Shalaev, V. M.; Grbic, A. Efficient light bending with isotropic metamaterial huygens' surfaces. *Nano Lett.* **2014**, *14*, 2491−2497.
(35) Kang, D.; Martinez, R. V.; Whitesides, G. M.; Tearney, G. J. Miniature grating for spectrally-encoded endoscopy. *Lab Chip* **2013**, *13*, 1810−1816.